Measurement Science and Technology

TECHNICAL NOTE • OPEN ACCESS

# LeXtender: a software package for advanced MOKE acquisition and analysis

To cite this article: Joachim Gräfe *et al* 2021 *Meas. Sci. Technol.* **32** 067002

OPEN ACCESS
IOP Publishing
Measurement Science and Technology
Meas. Sci. Technol. 32 (2021) 067002 (5pp)
https://doi.org/10.1088/1361-6501/abcdc0

## Technical Note

# LeXtender: a software package for advanced MOKE acquisition and analysis

**Joachim Gräfe, Felix Groß, Sven E Ilse, Daan B Boltje[1], Shreyas Muralidhar[2] and Eberhard J Goering**

Max Planck Institute for Intelligent Systems, Heisenbergstraße 3, Stuttgart 70569, Germany

E-mail: graefe@is.mpg.de

Received 2 September 2020, revised 31 October 2020
Accepted for publication 25 November 2020
Published 6 April 2021

**Abstract**

Contemporary scanning laser Kerr magnetometers are very efficient measurement devices that achieve very good signal to noise ratios and spatial resolution for magnetization measurements. When going beyond simple hysteresis loop measurements, large amounts of data can be acquired quickly and, thus, control software and automated processing becomes necessary to go beyond these simple measurements. Here, we present an open source software that realizes first-order reversal curves and magnetic property mapping based on scanning laser Kerr magnetometry. The modular software is easily extensible and provides a convenient user interface to make these more complex measurements accessible to a broader user base.

Keywords: MOKE, magnetometry, microscopy, force, imaging

(Some figures may appear in colour only in the online journal)

Magneto-optical Kerr effect (MOKE) measurements are based on the variations of the polarization of reflected light in dependence of the sample magnetization [1]. MOKE characterization is ubiquitous in laboratories dealing with magnetic materials, where it is mainly used for magnetometry and imaging of domain patterns [2–4]. With the development of faster MOKE hardware, more elaborate magnetometry schemes [5, 6] that go beyond simple hysteresis loop measurements have come into reach. However, advanced magnetometry methods require complex measurement routines and more computing power for their evaluation. Here, we present an open source software package that handles the fast acquisition and data analysis of first-order reversal curves (FORCs) and magnetic property mapping [7]. Both methods allow for the characterization of microscopic interactions: FORC by disentangling individual switching events and determining the coercive field and interaction field distributions [8–12]; and the latter by imaging the microscopic distributions of coercivity, (exchange) bias/interaction field, remanence and magnetization.

The software is implemented in MathWorks MATLAB using the Parallel Computing Toolbox. This enables parallel and distributed computing, depending on the complexity of the calculation. MOKE data is acquired using a Durham Magneto Optics NanoMOKE3 equipped with a 660 nm laser. The system is interfaced via text commands. In general, all methods are split into three modules: a graphical user interface (GUI) for acquisition, a GUI for data analysis and a data processing core. The encapsulation of the processing core

[1] Present address: Delmic B.V., Delft, The Netherlands.
[2] Present address: Gothenburg University, Gothenburg, Sweden.

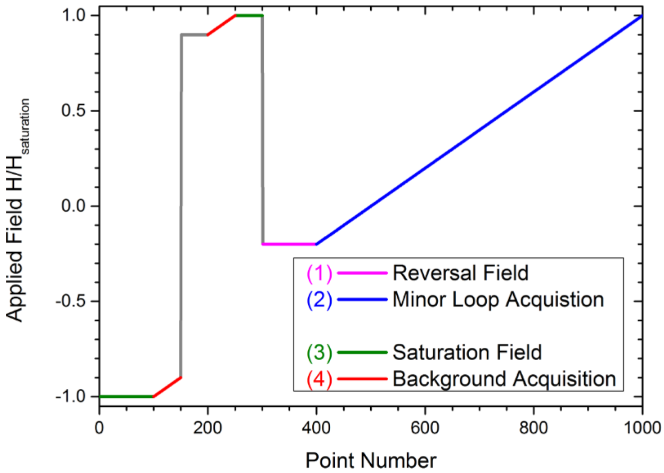


**Figure 1.** Field profile for first-order reversal curve (FORC) acquisition. The first part of the profile marked as (3) and (4) is used to calibrate the Kerr signal. The green parts (3) are used to compensate for drift and to normalize the Kerr signal to the saturation magnetization. The red parts (4) are used to compensate for the Faraday background of the signal. Subsequently, the reversal field is stabilized (1) and the actual minor loop (2) is measured. Reprinted from [13], with the permission of AIP Publishing.

allows for parametric and mass processing without user interaction.

## 1. First-order reversal curves

Previously, we have described the application of MOKE for FORC measurements [13]. In the following, we briefly discuss the software implementation to realize the acquisition and analysis of FORC diagrams.

### 1.1. *Acquisition*

To overcome drift and normalization issues, a specialized field profile is used for MOKE FORC, as shown in figure 1. The first part of the profile is used to calibrate the Kerr signal. The Kerr rotation in saturation is measured to normalize the Kerr signal to the saturation magnetization and the slope in saturation is measured to compensate for the Faraday background. Subsequently, the reversal field is stabilized and the actual minor loop is measured.

To acquire a set of minor loops this field profile is calculated for each reversal field and measured individually. When averaging multiple acquisition runs for a given reversal field, the full field profile is used for each run to account for continuous drift during the acquisition. Immediately after the acquisition of a minor loop the offset, normalization and background corrections are calculated and both the raw and processed minor loop are saved to a structured data array.

### 1.2. *Analysis*

Data analysis is implemented in a separate software module, because this task is computationally extensive when using conventional algorithms like FORCinel [14]. Thus, the GUI for analysis and the processing core are split to allow for batch calculation with different parameters like smoothing factor or data point interpolation. MOKE FORC data is unique in that it features more data points along the minor loop than conventional magnetometers can achieve. This results in numerical instabilities at the beginning of the individual minor loops. This is due to non-monotonous changes of the magnetic field caused by overshoots of the closed loop PID control of the magnetic field. This can be corrected without significant information loss by clipping the first data points of each minor loop. Furthermore, the modular design allows replacement of the processing core with modern GPU-accelerated algorithms like gFORC [15].

In general, the FORC density $\rho$ is defined as

$$\rho(H,H_r) \equiv -\frac{1}{2}\frac{\partial^2 \mathrm{M}(H,H_r)}{\partial H \partial H_r}, \qquad (1)$$

with the applied field $H$ and the reversal field $H_r$. Here, a variation of the FORCinel [14] algorithm is implemented for the calculation of $\rho$ from the experimental data. Because MOKE is a very fast measurement technique in comparison to VSM or SQUID, the software needs to be adapted to handle the large amount of measurement points. Thus, the first step is an interpolation to an equidistant grid. While this is inefficient for other magnetometers, it allows for a quick screening of the measurement data. The resulting matrix of reversal field $H_r$, applied field $H$ and magnetization $M$ is subsequently divided into subsets defined by the smoothing factor. A polynomial fit is used to calculate the FORC density, which is the computationally most demanding step. This is calculated in parallel for multiple data subsets. In our implementation, the number of parallel calculations is only limited by the number of available cores.

To illustrate results that can be achieved with LeXtender an example is shown in figure 2(a) [12]. There, alternating stripes with widths of 10 and 30 µm, and a length of 150 µm in 50 nm thick permalloy were measured. The two stripe widths result in two distinct peaks in the FORC diagram at different coercive fields. Additionally an interaction peak pair is observed due to the close proximity of the stripes (10 µm spacing). The full cycle of acquisition, evaluation and visualization of the FORC diagram were done in LeXtender.

## 2. Magnetic mapping

Laser Kerr magnetometers can be implemented on top of a scanning laser microscope [5, 6], like in the case of the Durham Magneto Optics NanoMOKE3 used here. Thus, several opportunities for imaging and property mapping arise. Beyond the mere reflectivity, hysteresis loops at several points can be measured and maps of magnetic properties like the coercivity, exchange bias, remanence and saturation can be extracted. In LeXtender this is achieved in two ways: a pixel-by-pixel acquisition where the laser is stabilized at each position and a full hysteresis is measured; a frame-by-frame approach were multiple Kerr images are measured at different fields. This is discussed in the following.

### *2.1. Pixel-by-pixel acquisition*

The most obvious solution for mapping out the magnetic properties is to stabilize the laser spot at each measurement position and measure a full hysteresis loop. While this is the most accurate approach to this problem, it is also the most time consuming. In this implementation, stabilizing the laser spot and driving the magnet coils are the limiting factors.

In our software implementation, the individual pixels are measured row-by-row. Experimentally, we found that more elaborate schemes yield little to no performance increase in the case of a scanning laser microscope with moderate field of view. For each pixel a full hysteresis loop is measured and averaged over several cycles if necessary. The characteristic parameters of the hysteresis are extracted and the individual data points are sorted into a position $x$, $y$, field $H$ and magnetization $M$ matrix.

### *2.2. Frame-by-frame acquisition*

A more time-efficient approach is to measure the Kerr rotation frame-by-frame, because laser scanning is fast in comparison to changing the magnetic field. In our experimental setup we can achieve dwell times per pixel and field of 13 µs and assume that similar MOKE setups can achieve a comparable speed. To achieve such short acquisition times a sufficient signal to noise ratio is important, because multi-loop averaging is not feasible. Thus, this approach is limited to materials with significant Kerr rotation.

The evaluation scheme that we employ in our software is shown in figure 3. Experimentally, a three-dimensional matrix of Kerr rotation (magnetization) in dependence of positions $x$, $y$ and the applied field $H$ is recorded. Subsequently, the matrix is split into individual pixels that are processed individually and in parallel. From the applied field $H$ the relative measurement time $t$ is calculated. For each, measurement spikes are detected and removed. These can be mostly attributed to vibrations and scanning issues. Subsequently, a time-dependent drift is removed, which can result from a slow mechanical drift of the sample. Afterwards, the measurement is transformed back to the field domain, i.e. magnetization in dependence of applied field $H$. An elliptical background is removed from this raw hysteresis to compensate higher-order magneto-optical effects. The raw hysteresis is split into two half-loops, i.e. a field sweep from positive to negative saturation and vice versa. For each half-loop a linear background in dependence of $H$ is removed to account for a linear Faraday background[3] and the zero offset is corrected. Subsequently, the characteristic parameters of the hysteresis are extracted, i.e. coercive field $H_c$, bias field $H_b$, saturation magnetization $M_{\mathrm{sat}}$, and a background corrected matrix $x$, $y$, $M$ is generated.

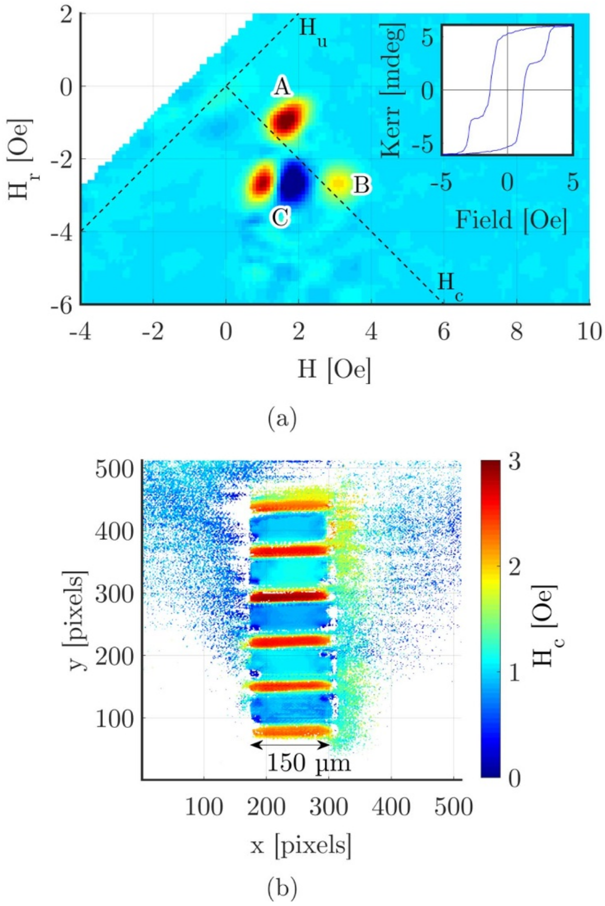


**Figure 2.** Example of results obtained with LeXtender adapted from [12]. The sample consists of 150 µm long and 50 nm thick permalloy stripes. These have alternating widths of 10 µm and 30 µm. (a) shows a FORC diagram with the FORC density $\rho$ plotted in dependence of the applied field $H$ and the reversal field $H_r$ and (b) shows a coercivity $H_c$ map that was acquired with the frame-by-frame approach.

An example of a sample measured with frame-by-frame acquisition is shown in figure 2(b). There the coercive field of the previously discussed sample with alternating stripes is mapped out. It is easily visible that the narrow stripes have a much higher coercivity than the wide stripes, as would be expected for such systems.

Because the frame-by-frame acquisition approach is optimized towards fast measurements, it is limited in sensitivity as the dwell time in our implementation is set to 13 µs per pixel and field value. Hence, in our experiments, a Kerr rotation of 5 mdeg was necessary to achieve reliable magnetic mapping in this operation mode. However, the dwell time is basically unlimited in the pixel-by-pixel approach, outlined above. Thus, this approach is more suitable for materials with low Kerr rotation, and we have achieved reliable results down to 0.1 mdeg of Kerr amplitude.

[3] This approach may be inaccurate for systems with oblique anisotropy or at very large fields due to non-linear Faraday background. Here, non-linear Faraday backgrounds were neglected, because of the moderate fields applied in our experiments. However, an additional background correction can easily be implemented into the LeXtender code.

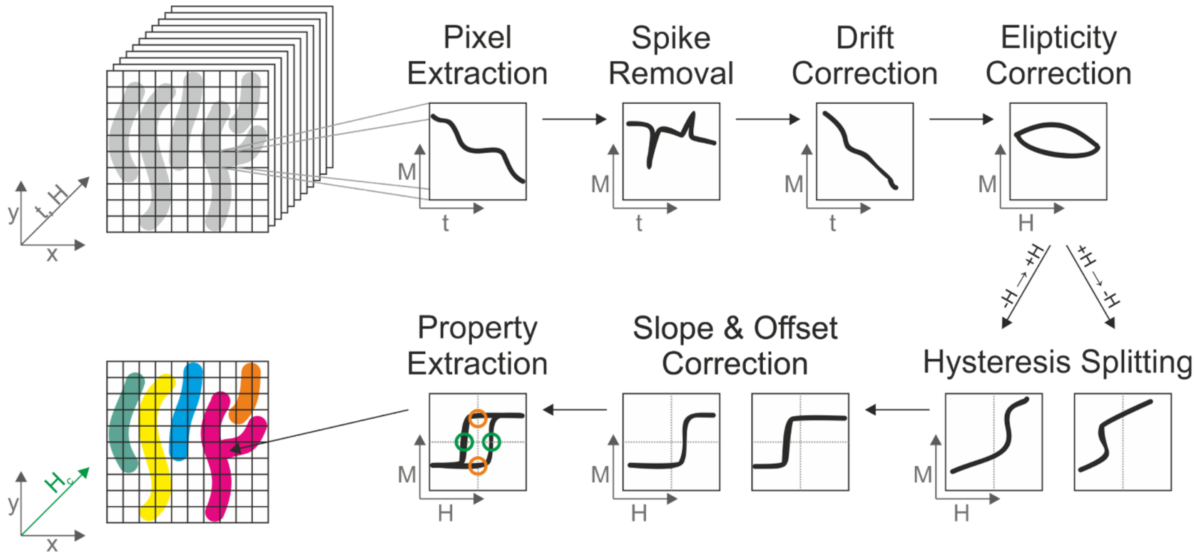


**Figure 3.** Schematic for the processing approach of frame-by-frame acquired magnetization data. Measurement-point-dependent magnetization traces are extracted pixel-by-pixel. Spikes and time dependent drift is removed. After transfer into the applied field domain, non-linear optical background effects that lead to an elliptical distortion are subtracted. Subsequently, hysteresis loops are split for ascending and descending field directions. These half hystereses are corrected for slope and offset and reunited to yield a full hysteresis loop. Characteristic properties of theses loops, like coercivity and remanence, are determined and assembled into a two dimensional map of sample properties.

## 3. Summary

In summary, we have developed a control and evaluation software that implements complex magnetometry for scanning laser Kerr microscopes that go beyond simple hysteresis measurements. For FORCs a field profile according to [13] and a processing core that is optimized for data measured by Kerr magnetometers is implemented. However, LeXtender also allows analyzing FORC data acquired with other techniques to be analyzed in the same GUI. Additionally, two approaches for magnetic property mapping are shown: one that is reliable but slow, and another that is optimized for fast measurements relying on frame-by-frame acquisition and subsequent data processing. On top of this modular and extensible software solution we provide a GUI for easy operation that opens up these techniques to a broader user base.

## Supplementary materials

The code discussed here can be found at https://gitlab.gwdg.de/MoKeteam/LeXtender/.

## Data availability statement

The data that support the findings of this study are available from the corresponding author upon reasonable request.

## Acknowledgment

Patrick Audehm is gratefully acknowledged for generating the waitbar artwork using POV-Ray.

## ORCID iDs

Joachim Gräfe https://orcid.org/0000-0002-4597-5923
Felix Groß https://orcid.org/0000-0002-2412-285X
Shreyas Muralidhar https://orcid.org/0000-0002-1045-6111

## References

[1] Kerr J 1877 On rotation of the plane of polarization by reflection from the pole of a magnet *Philosophical Magazine Series 5* **3** 321–43

[2] Kim W S, Aderholz M and Kleemann W 1993 Calibration of polar Kerr rotation and ellipticity measurements *Meas. Sci. Technol.* **4** 1275

[3] Schäfer R 2007 Investigation of domains and dynamics of domain walls by the magneto-optical kerr-effect *Handbook of Magnetism and Advanced Magnetic Materials* (Hoboken, NJ: Wiley)

[4] Soldatov I V and Schäfer R 2017 Advanced MOKE magnetometry in wide-field Kerr-microscopy *J. Appl. Phys.* **122** 153906

[5] Cormier M, Ferré J, Mougin A, Cromiéres J-P and Klein V 2008 High resolution polar Kerr magnetometer for nanomagnetism and nanospintronics *Rev. Sci. Instrum.* **79** 033706

[6] Flajšman L, Urbánek M, Křižáková V, Vaňatka M, Turčan I and Šikola T 2016 High-resolution fully vectorial scanning Kerr magnetometer *Rev. Sci. Instrum.* **87** 053704

[7] Gräfe J, Groß F, Ilse S E, Boltje D, Muralidhar S, Goering E J and Schütz G 2017 LeXtender (available at: https://gitlab.gwdg.de/dynamikstuttgart/LeXtender)

[8] Stancu A, Andrei P and Stoleriu L 2006 Magnetic characterization of samples using first- and second-order reversal curve diagrams *J. Appl. Phys.* **99** 08D702

[9] Fanny B, Louis-Philippe C, David M and Arthur Y 2010 Extracting individual properties from global behaviour: first-order reversal curve method applied to magnetic nanowire arrays *Electrodeposited Nanowires and Their Applications* (Rijeka: InTechOpen)
[10] Gräfe J *et al* 2016 Combined first-order reversal curve and x-ray microscopy investigation of magnetization reversal mechanisms in hexagonal antidot lattices *Phys. Rev.* B **93** 014406
[11] Gräfe J *et al* 2016 Geometric control of the magnetization reversal in antidot lattices with perpendicular magnetic anisotropy *Phys. Rev.* B **93** 104421
[12] Groß F, Ilse S E, Schütz G, Gräfe J and Goering E 2019 Interpreting first-order reversal curves beyond the Preisach model: an experimental permalloy microarray investigation *Phys. Rev.* B **99** 064401
[13] Gräfe J, Schmidt M, Audehm P, Schütz G and Goering E 2014 Application of magneto-optical Kerr effect to first-order reversal curve measurements *Rev. Sci. Instrum.* **85** 023901
[14] Harrison R J and Feinberg J M 2008 FORCinel: an improved algorithm for calculating first-order reversal curve distributions using locally weighted regression smoothing *Geochem. Geophys. Geosyst.* **9** 5
[15] Groß F, Martínez-García J C, Ilse S E, Schütz G, Goering E, Rivas M and Gräfe J 2019 gFORC: a graphics processing unit accelerated first-order reversal-curve calculator *J. Appl. Phys.* **126** 163901